

Enhanced light output of InGaN/GaN blue light emitting diodes with Ag nano-particles embedded in nano-needle layer

Lee-Woon Jang,¹ Jin-Woo Ju,² Dae-Woo Jeon,¹ Jae-Woo Park,¹ A. Y. Polyakov,¹ Seung-jae Lee,² Jong-Hyeob Baek,² Song-Mei Lee,³ Yong-Hoon Cho,³ and In-Hwan Lee^{1,*}

¹*School of Advanced Materials Engineering and Research Center of Advanced Materials Development and Semiconductor Physics Research Center, Chonbuk National University, Jeonju 561-756, Korea*

²*LED device team, Korea Photonics Technology Institute, Gwangju 500-779, Korea*

³*Department of Physics, Graduate School of Nanoscience & Technology (WCU), and KI for the Nano Century, KAIST, Daejeon, 305-701, Korea*

*ihlee@jbnu.ac.kr

Abstract: 2.7 times increase in room temperature photoluminescence (PL) intensity and 3.2 times increase in electroluminescence (EL) intensity were observed in blue multi-quantum-well (MQW) GaN/InGaN light emitting diodes (LEDs) as a result of introduction of nano-needle structure embedded with Ag nanoparticles (NPs) into n-GaN film underlying the active MQW region and thick p-GaN contact layer of LEDs. The nano-needle structure was produced by photoelectrochemical etching. Simultaneously a measurable decrease in room temperature decay time from 2.2 ns in control samples to 1.6 ns in PL was observed. The results are explained by strong coupling of recombination in GaN/InGaN MQWs with Ag NPs related localized surface plasmons.

©2012 Optical Society of America

OCIS codes: (240.6680) Surface plasmons; (250.5230) Photoluminescence; (250.5590) Quantum-well, -wire and -dot devices.

References and links

1. K. Okamoto, I. Niki, A. Shvartsner, Y. Narukawa, T. Mukai, and A. Scherer, "Surface-plasmon-enhanced light emitters based on InGaN quantum wells," *Nat. Mater.* **3**(9), 601–605 (2004).
2. M. K. Kwon, J. Y. Kim, B. H. Kim, I. K. Park, C. Y. Cho, C. C. Byeon, and S. J. Park, "Surface-plasmon-enhanced light-emitting diodes," *Adv. Mater. (Deerfield Beach Fla.)* **20**(7), 1253–1257 (2008).
3. D. M. Yeh, C. Y. Chen, Y. C. Lu, C. F. Huang, and C. C. Yang, "Formation of various metal nanostructures with thermal annealing to control the effective coupling energy between a surface plasmon and an InGaN/GaN quantum well," *Nanotechnology* **18**(26), 265402 (2007).
4. T. S. Oh, H. Jeong, Y. S. Lee, J. D. Kim, T. H. Seo, H. Kim, A. H. Park, K. J. Lee, and E. K. Suh, "Coupling of InGaN/GaN multiquantum-wells photoluminescence to surface plasmons in platinum nanocluster," *Appl. Phys. Lett.* **95**(11), 111112 (2009).
5. L. W. Jang, J. W. Ju, J. W. Jeon, D. W. Jeon, J. H. Choi, S. J. Lee, S. R. Jeon, J. H. Baek, E. Sari, H. V. Demir, H. D. Yoon, S. M. Hwang, and I. H. Lee, "Enhanced optical characteristics of light emitting diodes by surface plasmon of Ag nanostructures," *Proc. SPIE* **7945**, 794511 (2011).
6. C. Y. Cho, S. J. Lee, J. H. Song, S. H. Hong, S. M. Lee, Y. H. Cho, and S. J. Park, "Enhanced optical output power of green light-emitting diodes by surface plasmon of gold nanoparticles," *Appl. Phys. Lett.* **98**(5), 051106 (2011).
7. C. Y. Cho, M. K. Kwon, S. J. Lee, S. H. Han, J. W. Kang, S. E. Kang, D. Y. Lee, and S. J. Park, "Surface plasmon-enhanced light-emitting diodes using silver nanoparticles embedded in p-GaN," *Nanotechnology* **21**(20), 205201 (2010).
8. C. Y. Cho, K. S. Kim, S. J. Lee, M. K. Kwon, H. D. Ko, S. T. Kim, G. Y. Jung, and S. J. Park, "Surface plasmon-enhanced light-emitting diodes with silver nanoparticles and SiO₂ nano-disks embedded in p-GaN," *Appl. Phys. Lett.* **99**(4), 041107 (2011).
9. C. Youtsey, L. T. Romano, R. J. Molnar, and I. Adesida, "Rapid evaluation of dislocation densities in n-type GaN films using photoenhanced wet etching," *Appl. Phys. Lett.* **74**(23), 3537–3539 (1999).
10. I. Han, R. Datta, S. Mahajan, R. Bertram, E. Lindow, C. Werkhoven, and C. Arena, "Characterization of threading dislocations in GaN using low-temperature aqueous KOH etching and atomic force microscopy," *Sem. Mater.* **59**(11), 1171–1173 (2008).
11. C. F. Lin, C.-C. Yang, C.-M. Lin, K.-T. Chen, C.-W. Hu, and J.-D. Tsay, "InGaN-based light-emitting diodes with a multiple air gap layer," *Electrochem. Solid-State Lett.* **12**(10), H365–H368 (2009).

12. T. Izumi, Y. Narukawa, K. Okamoto, Y. Kawakami, S. Fujita, and S. Nakamura, "Time-resolved photoluminescence spectroscopy in GaN-based semiconductors with micron spatial resolution," *J. Lumin.* **87-89**, 1196–1198 (2000).
 13. M. S. Minsky, S. Watanabe, and N. Yamada, "Radiative and nonradiative lifetimes in GaInN/GaN multi-quantum wells," *J. Appl. Phys.* **91**(8), 5176–5181 (2002).
 14. F. Yun, Y. Fu, Y. T. Moon, U. Ozgur, J. Q. Xie, S. Dogan, H. Morkoc, C. K. Inoki, T. S. Kuan, L. Zhou, and D. J. Smith, "Reduction of threading dislocations in GaN overgrowth by MOCVD on TiN porous network templates," *Phys. Status Solidi., A Appl. Mater. Sci.* **202**(5), 749–753 (2005).
-

1. Introduction

Recent years have seen a growing interest in studying the effects of optical interaction between localized surface plasmons (LSPs) and GaN. This interest is largely fuelled by reports showing that strong coupling of LSPs and multi-quantum-well (MQW) regions of GaN-based structures can lead to a remarkable enhancement of the light intensity emitted by the structures due to a very efficient energy transfer from electrons and holes recombining in the MQW region to the excited states of LSPs (fundamentals of the process and relevant references to earlier work can be found e.g. in [1–4]). As a result, the internal quantum efficiency of the structures can be significantly improved at the expense of suppressing the non-radiative recombination contribution (see e.g. [1]). For GaN MQW structures emitting in the blue spectral region the resonant LSP coupling is easily achieved by Ag nanoparticles (NPs) layers and effective energy re-pumping from non-radiative channel into the LSP optical modes has been convincingly demonstrated for GaN/InGaN MQW light emitting diodes (LEDs, see e.g. [3]). However, for the LSP enhancement to be efficient, the NP layer should be placed in close proximity to the active MQW region of the device, generally no further than 40–50 nm (see e.g. [1]). This seriously complicates the practical application of the effect because, in GaN-based LEDs, the thickness of the top contact p-GaN layer should exceed about 70–80 nm to provide well behaved p-n junction performance and good current spreading [2].

Several approaches have been tried to alleviate this problem. In [5] it was shown that by creating a surface roughening of the suitably thick p-GaN spacer layer and by placing Ag NPs inside the "pockets" of the roughened structure the LSPs can be brought sufficiently close to the MQW region to cause a serious increase in the LED quantum efficiency. Unfortunately, the technology is very challenging both in terms of obtaining the right thickness of residual p-GaN spacer under Ag NPs and in terms of obtaining low ohmic contact series resistance to the nanostructured p-type contact layer.

Another approach described in recent papers [6,7] involves deposition of Ag NPs on a thin p-GaN layer on top of the active MQW structure with subsequent regrowth by p-GaN to the required thickness. Further improvement of structural and electrical characteristics could be obtained by masking the Ag NPs with SiO₂ nanodiscs before the overgrowth stage. In that case the structural characteristics were greatly improved due to epitaxial lateral overgrowth (ELO) over the Ag/SiO₂ pattern [8]. Despite the obvious success of this approach it requires very careful optimization of the overgrowth conditions and SiO₂ microdiscs deposition conditions.

In what follows we describe an alternative approach in which a shallow nano-needle structure is created by photo-electrochemical (PEC) etching in n-GaN, Ag NPs are deposited on this nano-needle structure and the structure is then overgrown by a thin n-GaN film with subsequent growth of the MQW and p-GaN regions as in standard LEDs.

2. Experimental methods

The InGaN/GaN MQW structure was grown by metal organic chemical vapor deposition (MOCVD) technique as described in [5], with the main difference being the growth interruption after depositing a 1 μm thick undoped GaN layer and a 2 μm thick n-type GaN layer grown at 1060 °C. The PEC etching of this template structure was performed in 0.02 M KOH solution for 30 min at anodic voltage of 2 V [9]. The light source was a UV-enhanced xenon lamp with a power density of 350 mW/cm². A 20 nm thick Ag film was deposited on

the PEC etched surface by e-beam evaporator. Then, n-type GaN film with intended thickness of 50 nm was grown at a temperature of 850°C. This layer was grown over by the MQW region consisting of 5 GaN/InGaN QWs and after that by the p-GaN contact layer. The GaN barriers (10 nm) and InGaN wells (2 nm) were grown at temperatures of 850 °C and 750 °C, respectively. The thickness of the p-type GaN layer was 150 nm. Characteristic dimensions of GaN nano-needles and of Ag NPs were determined by using scanning electron microscopy (SEM). Structural characterization involved high resolution x-ray diffraction (HRXRD) measurement in triple-axis geometry. Atomic force microscopy (AFM) measurements were performed to study the surface morphology and assess the dislocation density. Photoluminescence (PL) and electroluminescence (EL) measurements were carried out to study the optical and electrical properties of the structures. A 25mW, He-Cd laser (325nm) was used as the excitation source for the room temperature (RT) PL measurements. The EL characteristics were measured by a front-side photo detector with on-wafer probing of the devices. In addition, time resolved PL (TRPL) measurements (using PicoQuant PicoHarp 300) were performed at RT as described in [2,5]. The results of these measurements were compared for nano-needle LED structures embedded with Ag NPs and for control LED structure without such layers.

3. Results and discussion

The schematic diagram (left) of the process flow, corresponding SEM images (center) and photograph (right) are shown in Fig. 1. Nano-needles with diameter of 10-30 nm, length of 300 nm and the pitch of about 100 nm were formed after PEC etching of n-GaN (Fig. 1(b)). Figure 1(c) shows the Ag coated nano-needle structure observed after e-beam evaporation. The coating Ag layer was annealed in the GaN re-growth process so that Ag was preserved only near the bottom of the nano-needles, thus forming the Ag NPs network to be used in LSP coupling with the MQW region above. Experiments with satellite samples without regrowth showed that Ag NPs were preserved on top of GaN nano-needles for annealing at 600°C, but fell into the interneedle “pockets” at annealing temperature of 750°C. Hence this pre-annealing was included as a standard procedure preceding re-growth. To observe the Ag NP shape on PEC etched layer after annealing, the Ag deposited sample was taken out without the re-growth of GaN in MOCVD. In the SEM image shown in Fig. 1(c), the nano-needles formed around threading dislocations [9] are highlighted by dashed white circles. The light and shaded features outside the nano-needles are produced by the agglomerated Ag layer. As a reference we used the sample without PEC etching and Ag deposition, but with other layers (50 nm n-GaN, MQW region, the contact top p-GaN film) grown under exactly the same conditions, including the lowered temperature during the 50-nm-thick n-GaN layer deposition (d). After the re-growth of LED structure, we compared the reference, re-grown sample after Ag deposition with PEC and without PEC (e). The Ag embedded sample without PEC shows a slightly gray color, while the sample with PEC shows a more dark gray color. This indicates that the nano-needle structures can hold the Ag NPs better than when they are deposited on flat surface and regrown by MOCVD. This is corroborated by PL intensity comparison for the reference sample and the sample with Ag NPs prepared on the flat surface and regrown. We observed in that case the deterioration of PL intensity for the Ag NP sample, in contrast to the results for the nano-needle sample with Ag NPs. Our explanation is that the NPs are confined in the latter case to the pockets of the nano-needle structure whilst the tops of the nano-needles present a platform for selective lateral overgrowth.

The Structural perfection and crystalline quality of the PEC etched and embedded sample and the control sample is compared using the HRXRD patterns [2] and AFM measurements after etching in 45% KOH:H₂O aqueous solution [10] of these two samples. The position and the half-width of the 0th order diffraction peak and the number and angular position of the QW related side fringes are very similar which indicates the similar In composition in QWs and the sharpness of the GaN/InGaN interfaces was not strongly affected by the PEC etching and Ag deposition [2].

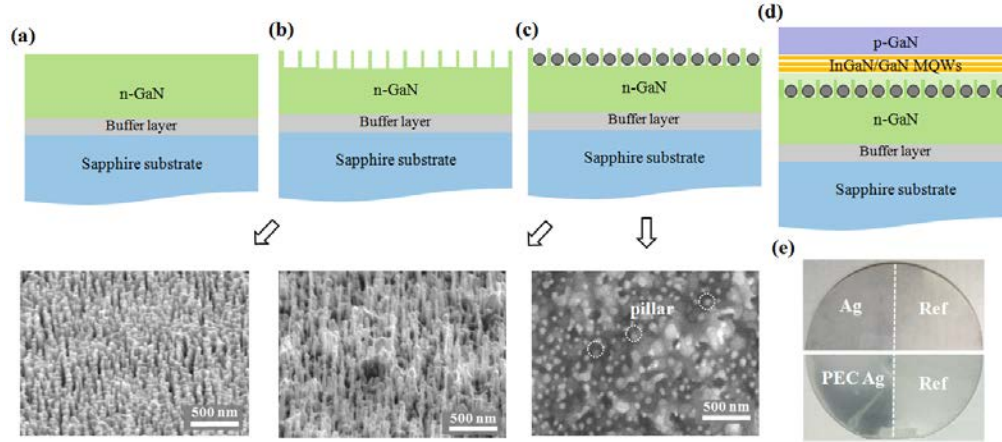


Fig. 1. Schematic fabrication process of the Ag embedded sample after PEC wet etching (left) and the SEM images of each processes (right); (a) GaN template before PEC etching, (b) nano-needle structure and SEM image after PEC, (c) Ag deposition on nano-needle structure, (d) re-grown LED sample, (e) photograph of re-grown LED.

In addition, Fig. 2 presents the results of AFM scanning for the samples with and without PEC etching and Ag deposition. Dislocations in the figure are revealed as small nanometer size pits. The pit density that is associated with the threading dislocations (TD) density was found to be $1.6 \times 10^{10}/\text{cm}^2$ for the sample without Ag (Fig. 2(a)) and considerably lower, $3 \times 10^9/\text{cm}^2$ (Fig. 2(b)) for the nanostructured sample with Ag NPs. The decrease in the TD density in the PEC etched sample with Ag is ascribed by us to ELO-type re-growth process in which the surface patterned by etching serves as a nanomask similarly to growth on nanopatterned GaN [11].

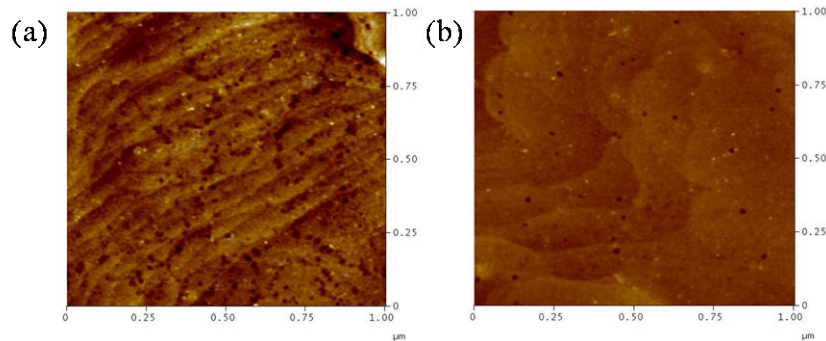


Fig. 2. AFM image of control sample (a) and Ag embedded sample (b). The scan area is $1 \mu\text{m} \times 1 \mu\text{m}$.

Electrical and optical properties of control and PEC etched, Ag embedded structures are compared in Fig. 3. Current-voltage I-V characteristics (a) of these LEDs were qualitatively and quantitatively very similar, with the turn-on voltages close to 4V at 20 mA in both cases. At the same time, the reverse current of the Ag-embedded sample was decreased by almost an order of magnitude, most likely due to the decreased dislocation density that seems to overpower in our case possible detrimental effects of Ag incorporation. In contrast to the similarity in forward I-V characteristics, the light output power (b) of the PEC etched, Ag embedded sample was found to be 3.2 times higher at 100 mA compared to control sample. Room temperature PL spectra (c) showed almost the same MQW PL peak position (the peak was slightly red-shifted by about 4 nm due to the interaction with LSPs with absorbance spectra peaked near 455 nm), but the peak magnitude was 2.7 times higher for the Ag embedded sample.

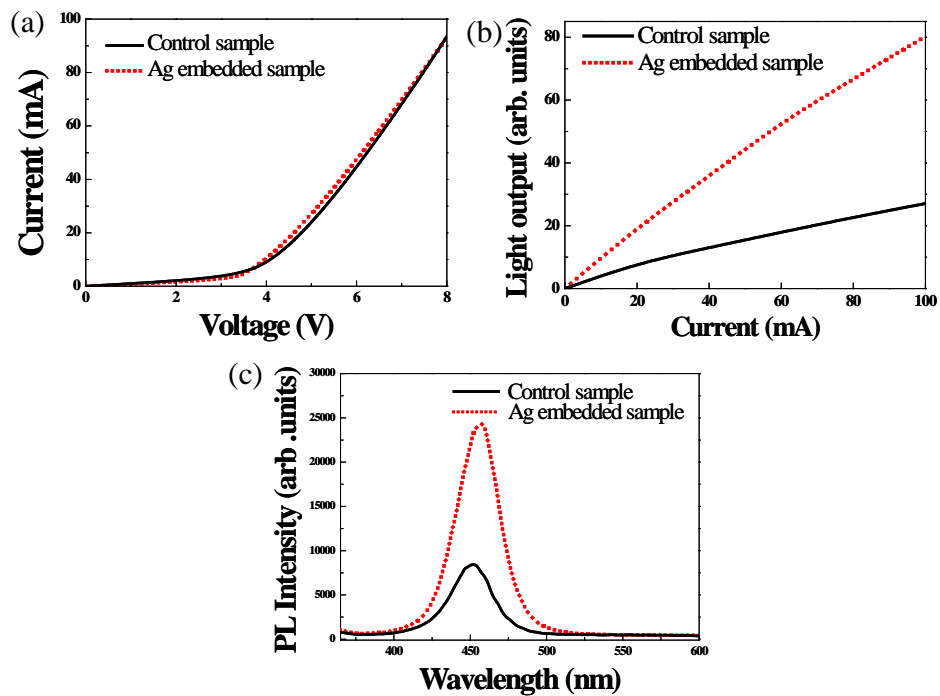


Fig. 3. Current-voltage characteristics (a), optical output power versus driving current characteristics (b) and room temperature PL spectra of InGaN/GaN MQW LED of control (black line) and Ag embedded sample (red dotted line).

Finally, Fig. 4 compares the TRPL decay curves for PL peak energies for the control and the Ag embedded samples. Numeric fitting gave for the fast-time decay components of the relaxation curves characteristic lifetimes of 1.6 ns for the Ag embedded sample and 2.2 ns for the control sample. It is known that dislocations in GaN act as efficient centers of non-radiative recombination [12–14], which should have increased the recombination time in the PEC etched and Ag embedded sample due to the lower dislocation density. The fact that in reality the relaxation time in this sample is shorter than in the control sample can be attributed to efficient transfer of energy from MQW region to the LSP states while at the same time increasing the PL and EL intensity in the Ag embedded nano-needle sample [2,4,5]. The question of relative impacts on EL and PL enhancement of the dislocation density decrease and of LSP coupling in this sample compared to the control sample is rather complicated. Our preliminary analysis based on the comparison of EL enhancement in the Ag embedded sample on the driving forward current suggests that, at low forward currents, the effect of structural improvement dominates, whereas at high injection level the enhancement due to LSP coupling becomes predominant. But this question needs more detailed study.

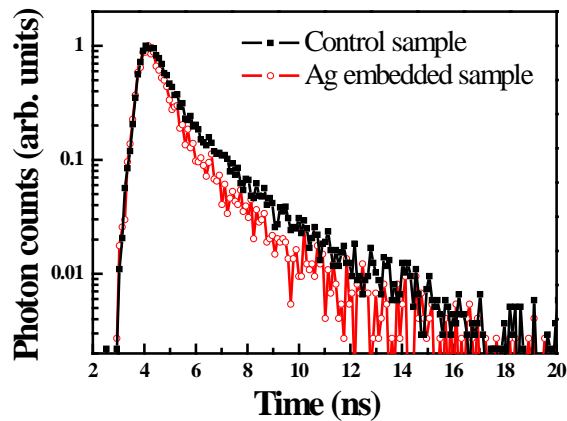


Fig. 4. Room temperature PL relaxation curves for the peak PL energy for the control sample (solid squares, black) and PEC etched, Ag embedded sample (open circles, red) at room temperature.

4. Conclusion

Therefore, we have shown that PEC etching of the n-GaN template and Ag deposition prior to deposition of thin 50 nm n-GaN re-growth layer and growth of the GaN/InGaN MQW region and p-GaN cap is a viable way to provide good coupling of Ag NP LSPs with MQWs and to measurably enhance the luminescence efficiency both with optical and electrical injection. Compared to the approach described in [6–8] the technology discussed above has the potential advantage of getting rid of energy losses in metallic NPs in front-surface emission. Clearly, more work is required before the true potential of the technological approach outlined in the present paper will be realized. These studies are currently underway in our laboratories.

Acknowledgments

This work was supported by the National Research Foundation of Korea (NRF) funded by the Korea government (MEST) (2010-0019626, 2010-0026614).